Jets Lecture 7

Tuomas Savolainen
Max-Planck-Institut für Radioastronomie, Bonn, Germany

tsavolainen@mpifr.de

Autumn 2011

Outline

1. Jet acceleration and collimation
2. Jet launching
3. Matter content in jets

Jet acceleration and collimation

Jet acceleration and collimation

- Launching a jet requires 1) strong negative outward pressure gradient and 2) a confinement mechanism

Jet acceleration and collimation

- Launching a jet requires 1) strong negative outward pressure gradient and 2) a confinement mechanism
- Acceleration/collimation likely takes place over an extended region in the jet: from a few R_g to $10^3 - 10^5 R_g$

Jet acceleration and collimation

- Launching a jet requires 1) strong negative outward pressure gradient and 2) a confinement mechanism
- Acceleration/collimation likely takes place over an extended region in the jet: from a few R_g to $10^3 - 10^5 R_g$
- Hydrodynamic jet: acceleration by conversion of internal energy into bulk flow and collimation by thick-walled funnel or hot accretion disk wind

Jet acceleration and collimation

- Launching a jet requires 1) strong negative outward pressure gradient and 2) a confinement mechanism
- Acceleration/collimation likely takes place over an extended region in the jet: from a few R_g to $10^3 - 10^5 R_g$
- Hydrodynamic jet: acceleration by conversion of internal energy into bulk flow and collimation by thick-walled funnel or hot accretion disk wind
- Magnetohydrodynamic jet: acceleration by magnetic pressure and collimation by magnetic hoop stress

Hydrodynamic acceleration and collimation

- If the pressure of the ISM drops by many orders of magnitude from the central regions, ∇p provides acceleration (according to relativistic Bernoulli equation)

Hydrodynamic acceleration and collimation

- If the pressure of the ISM drops by many orders of magnitude from the central regions, ∇p provides acceleration (according to relativistic Bernoulli equation)
- Internal energy is converted to bulk kinetic energy

Hydrodynamic acceleration and collimation

- If the pressure of the ISM drops by many orders of magnitude from the central regions, ∇p provides acceleration (according to relativistic Bernoulli equation)
- Internal energy is converted to bulk kinetic energy
- Acceleration continues until $\Gamma \approx \frac{u_0}{\rho_0 c^2} = \langle \gamma_0 \rangle$. Therefore, high Γ requires ultrarelativistic plasma in the central engine

Hydrodynamic acceleration and collimation

- If the pressure of the ISM drops by many orders of magnitude from the central regions, ∇p provides acceleration (according to relativistic Bernoulli equation)
- Internal energy is converted to bulk kinetic energy
- Acceleration continues until $\Gamma \approx \frac{u_0}{\rho_0 c^2} = \langle \gamma_0 \rangle$. Therefore, high Γ requires ultrarelativistic plasma in the central engine
- Mechanical collimation to $\phi < 1^\circ$ requires large external pressure in the collimation zone

Hydrodynamic acceleration and collimation

- If the pressure of the ISM drops by many orders of magnitude from the central regions, ∇p provides acceleration (according to relativistic Bernoulli equation)
- Internal energy is converted to bulk kinetic energy
- Acceleration continues until $\Gamma \approx \frac{u_0}{\rho_0 c^2} = \langle \gamma_0 \rangle$. Therefore, high Γ requires ultrarelativistic plasma in the central engine
- Mechanical collimation to $\phi < 1^\circ$ requires large external pressure in the collimation zone
- Probably the most favourable case: external medium is an isothermal, constant-velocity wind from the accretion disk. However, significant problem with the inferred X-ray luminosity from the hot wind well exceeding observed values.

Magnetic acceleration and collimation

- Toroidal component of the B-field can provide both: acceleration (via magnetic pressure gradient) and collimation (via hoop stress)

Magnetic acceleration and collimation

- Toroidal component of the B-field can provide both: acceleration (via magnetic pressure gradient) and collimation (via hoop stress)
- Requires wound-up B-field with higher energy density than the kinetic energy density of the particles (Poynting-flux dominated jet). Mostly toroidal B-field can be a consequence of B-field being anchored in a differentially rotating accretion disk or in the ergosphere of a rotating BH.

Magnetic acceleration and collimation

- Toroidal component of the B-field can provide both: acceleration (via magnetic pressure gradient) and collimation (via hoop stress)
- Requires wound-up B-field with higher energy density than the kinetic energy density of the particles (Poynting-flux dominated jet). Mostly toroidal B-field can be a consequence of B-field being anchored in a differentially rotating accretion disk or in the ergosphere of a rotating BH.
- $\sim 1/2$ of magnetic energy is converted to flow energy if $\frac{B}{\sqrt{4\pi\rho c^2}} >> 1 \rightarrow$ acceleration and collimation can continue out to $\sim 10^5 R_g$

Magnetic acceleration and collimation

- Toroidal component of the B-field can provide both: acceleration (via magnetic pressure gradient) and collimation (via hoop stress)
- Requires wound-up B-field with higher energy density than the kinetic energy density of the particles (Poynting-flux dominated jet). Mostly toroidal B-field can be a consequence of B-field being anchored in a differentially rotating accretion disk or in the ergosphere of a rotating BH.
- $\sim 1/2$ of magnetic energy is converted to flow energy if $\frac{B}{\sqrt{4\pi\rho c^2}} >> 1 \rightarrow$ acceleration and collimation can continue out to $\sim 10^5 R_g$
- Toroidal field requires current. There must be a return current as well, which will cause dissipation of energy where it crosses the field lines near the base of the flow.

Magnetic acceleration and collimation

- Toroidal component of the B-field can provide both: acceleration (via magnetic pressure gradient) and collimation (via hoop stress)
- Requires wound-up B-field with higher energy density than the kinetic energy density of the particles (Poynting-flux dominated jet). Mostly toroidal B-field can be a consequence of B-field being anchored in a differentially rotating accretion disk or in the ergosphere of a rotating BH.
- $\sim 1/2$ of magnetic energy is converted to flow energy if $\frac{B}{\sqrt{4\pi \rho c^2}} >> 1 \rightarrow$ acceleration and collimation can continue out to $\sim 10^5 R_g$
- Toroidal field requires current. There must be a return current as well, which will cause dissipation of energy where it crosses the field lines near the base of the flow.
- Current-carrying jets are unstable against current-driven helical (kink) instability

Magnetic acceleration and collimation

- Toroidal component of the B-field can provide both: acceleration (via magnetic pressure gradient) and collimation (via hoop stress)
- Requires wound-up B-field with higher energy density than the kinetic energy density of the particles (Poynting-flux dominated jet). Mostly toroidal B-field can be a consequence of B-field being anchored in a differentially rotating accretion disk or in the ergosphere of a rotating BH.
- $\sim 1/2$ of magnetic energy is converted to flow energy if $\frac{B}{\sqrt{4\pi \rho c^2}} >> 1 \rightarrow$ acceleration and collimation can continue out to $\sim 10^5 R_g$
- Toroidal field requires current. There must be a return current as well, which will cause dissipation of energy where it crosses the field lines near the base of the flow.
- Current-carrying jets are unstable against current-driven helical (kink) instability
- Works in the new, fully self-consistent 3D GRMHD simulations of jet launching from an accretion flow

Jet launching

Launching magnetic jet from an accretion disk (Blandford & Payne 1982)

- Assume magnetic field anchored in differentially rotating accretion disk – kinetic energy of rotation exceeds $B^2/8\pi$ and field lines corotate with the disk.

From Spruit (2010)

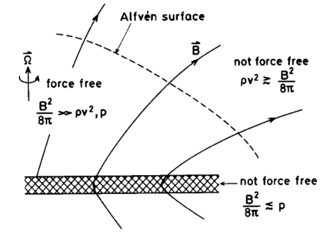

Launching magnetic jet from an accretion disk (Blandford & Payne 1982)

- Assume magnetic field anchored in differentially rotating accretion disk – kinetic energy of rotation exceeds $B^2/8\pi$ and field lines corotate with the disk.
- Above and below the disk magnetic pressure dominates forcing gas flow to follow the field lines corotating with the disk $\rightarrow$ if field lines are tilted wrt axial direction, centrifugal acceleration follows

From Spruit (2010)

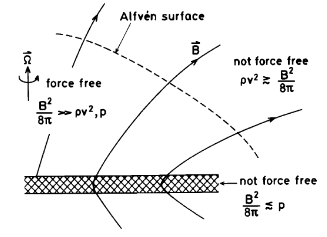

Launching magnetic jet from an accretion disk (Blandford & Payne 1982)

- Assume magnetic field anchored in differentially rotating accretion disk – kinetic energy of rotation exceeds $B^2/8\pi$ and field lines corotate with the disk.
- Above and below the disk magnetic pressure dominates forcing gas flow to follow the field lines corotating with the disk $\rightarrow$ if field lines are tilted wrt axial direction, centrifugal acceleration follows
- As the flow accelerates and field strength decreases, the approximation of rigid corotation of the gas with the field lines stops being valid – this happens at Alfvén radius where flow speed $= B/\sqrt{4\pi\rho}$

From Spruit (2010)

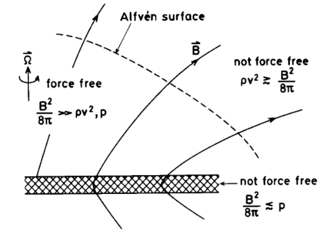

Launching magnetic jet from an accretion disk (Blandford & Payne 1982)

- At the Alfvén point the field lines start lagging behind and the B-field gets wound-up into a helix

From Spruit (2010)

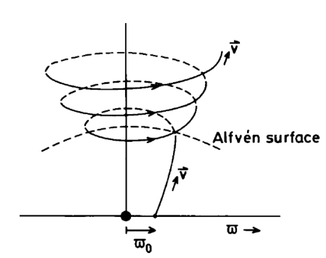

Launching magnetic jet from an accretion disk (Blandford & Payne 1982)

- At the Alfvén point the field lines start lagging behind and the B-field gets wound-up into a helix
- Beyond the Alfvén point the jet is accelerated by the gradient in the magnetic pressure of the toroidal component of the B-field and collimated by hoop stress

From Spruit (2010)

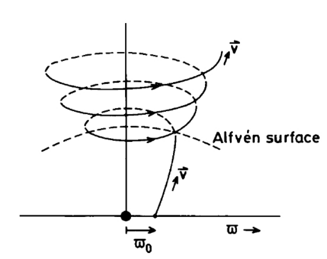

Launching magnetic jet from an accretion disk (Blandford & Payne 1982)

- At the Alfvén point the field lines start lagging behind and the B-field gets wound-up into a helix
- Beyond the Alfvén point the jet is accelerated by the gradient in the magnetic pressure of the toroidal component of the B-field and collimated by hoop stress
- Collimation and acceleration can continue until half of the magnetic flux is converted into kinetic flux

From Spruit (2010)

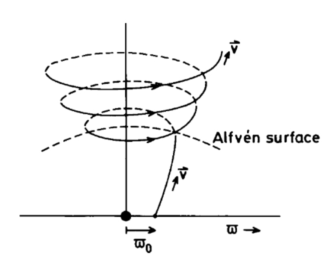

Launching magnetic jet from a rotating BH (Blandford & Znajek 1977)

- Magnetically accelerated jet can also be launched from a rotating black hole threaded by B-field (provided by accretion disk)

Hirose et al. (2004)

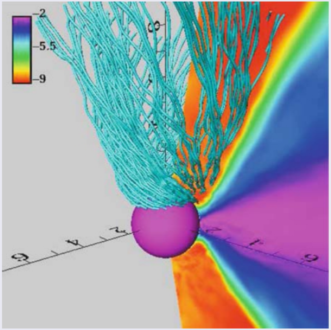

Launching magnetic jet from a rotating BH (Blandford & Znajek 1977)

- Magnetically accelerated jet can also be launched from a rotating black hole threaded by *B*-field (provided by accretion disk)
- Near the rotating black hole "frame dragging" – a GR effect – makes even particles with zero angular momentum to rotate around BH

Hirose et al. (2004)

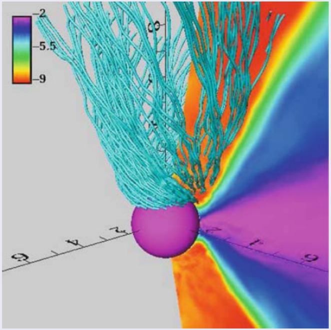

Launching magnetic jet from a rotating BH (Blandford & Znajek 1977)

- Magnetically accelerated jet can also be launched from a rotating black hole threaded by *B*-field (provided by accretion disk)
- Near the rotating black hole "frame dragging" – a GR effect – makes even particles with zero angular momentum to rotate around BH
- Now poloidal *B*-field lines in the ergosphere experience forced rotation making up a toroidal field component which can create Poynting flux that carries (BH's rotational) energy out to infinity

Hirose et al. (2004)

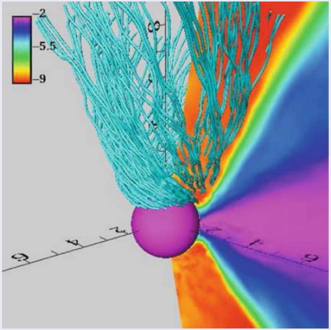

Launching magnetic jet from a rotating BH (Blandford & Znajek 1977)

- Magnetically accelerated jet can also be launched from a rotating black hole threaded by *B*-field (provided by accretion disk)
- Near the rotating black hole "frame dragging" – a GR effect – makes even particles with zero angular momentum to rotate around BH
- Now poloidal *B*-field lines in the ergosphere experience forced rotation making up a toroidal field component which can create Poynting flux that carries (BH's rotational) energy out to infinity
- Efficient way of extracting BH rotational energy and creating Poynting flux jets

Hirose et al. (2004)

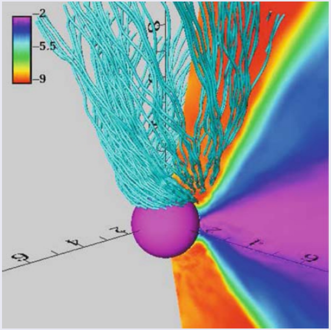

3D GRMHD simulations of jet launching

- State-of-art 3D GRMHD simulations show Blandford-Znajek mechanism at work and also demonstrate self-consistent launching of a jet from a system of spinning BH surrounded by magnetized accretion disc

McKinney & Blandford (2009)

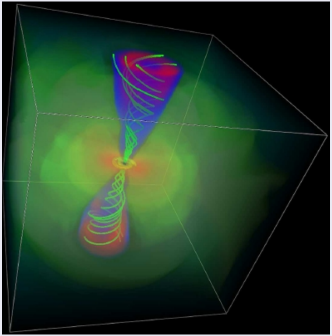

3D GRMHD simulations of jet launching

- State-of-art 3D GRMHD simulations show Blandford-Znajek mechanism at work and also demonstrate self-consistent launching of a jet from a system of spinning BH surrounded by magnetized accretion disc
- McKinney & Blandford (2009) showed that in an accreting dipolar B-field case, a $\Gamma \sim 10$ jet can be generated that is stable up to $10^3 R_g$! A rotating BH is required for generating high Lorentz factor outflows.

McKinney & Blandford (2009)

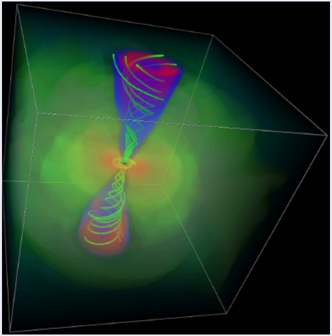

3D GRMHD simulations of jet launching

- State-of-art 3D GRMHD simulations show Blandford-Znajek mechanism at work and also demonstrate self-consistent launching of a jet from a system of spinning BH surrounded by magnetized accretion disc
- McKinney & Blandford (2009) showed that in an accreting dipolar B-field case, a $\Gamma \sim 10$ jet can be generated that is stable up to $10^3 R_g$! A rotating BH is required for generating high Lorentz factor outflows.
- Only mild helical structures due to kink instability are present in the simulation. Disc turbulence seems to be the main cause of jet sub-structure.

McKinney & Blandford (2009)

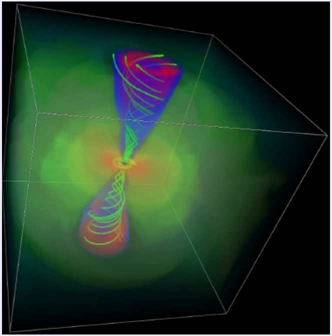

3D GRMHD simulations of jet launching

- State-of-art 3D GRMHD simulations show Blandford-Znajek mechanism at work and also demonstrate self-consistent launching of a jet from a system of spinning BH surrounded by magnetized accretion disc
- McKinney & Blandford (2009) showed that in an accreting dipolar B-field case, a $\Gamma \sim 10$ jet can be generated that is stable up to $10^3 R_g$! A rotating BH is required for generating high Lorentz factor outflows.
- Only mild helical structures due to kink instability are present in the simulation. Disc turbulence seems to be the main cause of jet sub-structure.
- Accreting quadrupolar B-field does not produce strong outflows in these simulations

McKinney & Blandford (2009)

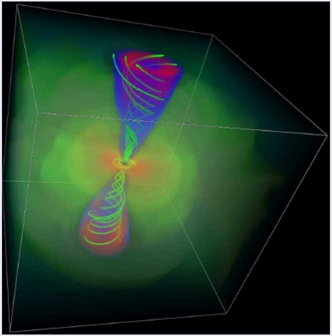

Movie of 3D GRMHD simulation

Connection between the jet and the central engine

- Accretion process itself can be driven by magneto-rotational turbulence, which is able to generate strong B-fields in the disk – a prerequisite to magnetic jet launching
- It is therefore expected that accretion and jet launching are significantly connected processes
- Connection between accretion disk state and jet production seen in XRBs
- Hints of similar connection in radio galaxy 3C120

Jet-disk coupling in 3C120 (Marscher et al. 2002)

- Dips in RXTE X-ray light curve observed four times just before and ejection of a new superluminal feature in the jet. Confirmed by Chatterjee et al. (2009) using more data.
- Similar behaviour as in XRBs – X-ray dips might be sign of the innermost part of the accretion disk disappearing beyond the event horizon
- Delay between the dips and emergence of new superluminal features gives a minimum distance of 0.3 pc between the VLBI core and the BH

Marscher et al. (2002)

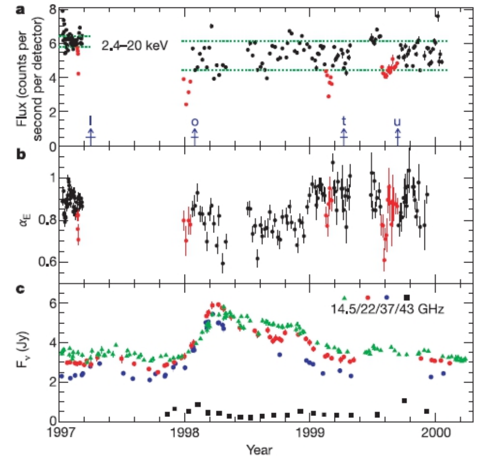

Conversion from Poynting-flux to kinetic flux

- The kpc-scale jets / radio lobes are consistent with being kinetic flux dominated

Conversion from Poynting-flux to kinetic flux

- The kpc-scale jets / radio lobes are consistent with being kinetic flux dominated
- If a jet starts as Poyting flux -dominated, there has to be a transition region

Conversion from Poynting-flux to kinetic flux

- The kpc-scale jets / radio lobes are consistent with being kinetic flux dominated
- If a jet starts as Poyting flux -dominated, there has to be a transition region
- How far from the BH this transition region is located? Theoretical arguments give ranges from $10^2 - 10^5 R_g$. Some observations indicate $10^3 R_g$, but recently we have seen flow acceleration upto $10^5 R_g$ in the MOJAVE survey

Matter content in jets

What are the jets made of?

- Normal plasma ($e^{-} - p^{+}$) or pair plasma ($e^{-} - e^{+}$) or combination of both?

What are the jets made of?

- Normal plasma ($e^- - p^+$) or pair plasma ($e^- - e^+$) or combination of both?
- Theoretically one would expect a jet launched from the accretion disk to consist mainly of normal plasma

What are the jets made of?

- Normal plasma ($e^- - p^+$) or pair plasma ($e^- - e^+$) or combination of both?
- Theoretically one would expect a jet launched from the accretion disk to consist mainly of normal plasma
- However, fast Poynting flux dominated flow from rotating BH may consist of pair plasma (created by pair production from high energy photons with jet B-field)

What are the jets made of?

- Normal plasma ($e^- - p^+$) or pair plasma ($e^- - e^+$) or combination of both?
- Theoretically one would expect a jet launched from the accretion disk to consist mainly of normal plasma
- However, fast Poynting flux dominated flow from rotating BH may consist of pair plasma (created by pair production from high energy photons with jet B-field)
- So far, we do not have any direct evidence for either case and the indirect evidence are contradictory

511 keV annihilation line

- Observing the 511 keV annihilation line from a jet would be a direct proof of pairs present in the jet

511 keV annihilation line

- Observing the 511 keV annihilation line from a jet would be a direct proof of pairs present in the jet
- The problem is that this line is extremely difficult to detect, because

511 keV annihilation line

- Observing the 511 keV annihilation line from a jet would be a direct proof of pairs present in the jet
- The problem is that this line is extremely difficult to detect, because
  - The cross-section for annihilation is relatively small for highly relativistic pairs
  - The line width can be broadened beyond recognition due to the high velocities
  - Current detectors are still relatively insensitive at this energy range

511 keV annihilation line

- Observing the 511 keV annihilation line from a jet would be a direct proof of pairs present in the jet
- The problem is that this line is extremely difficult to detect, because
  - The cross-section for annihilation is relatively small for highly relativistic pairs
  - The line width can be broadened beyond recognition due to the high velocities
  - Current detectors are still relatively insensitive at this energy range
- If we can find a source where jet-ISM interaction thermalizes the positrons, a narrow annihilation line could become detectable

Circular polarization and the case of 3C279

- Wardle et al. (1998) observed relatively high amount of circular polarization in the parsec-scale jet of 3C279

Circular polarization and the case of 3C279

- Wardle et al. (1998) observed relatively high amount of circular polarization in the parsec-scale jet of 3C279
- They attributed it to Faraday conversion requiring $\gamma_{\rm min} \lesssim 20$

Circular polarization and the case of 3C279

- Wardle et al. (1998) observed relatively high amount of circular polarization in the parsec-scale jet of 3C279
- They attributed it to Faraday conversion requiring $\gamma_{\rm min} \lesssim 20$
- Combining this with the requirement that intrinsic Faraday rotation does not completely depolarize the jet then leads to mostly pair-plasma dominated jet

Circular polarization and the case of 3C279

- Wardle et al. (1998) observed relatively high amount of circular polarization in the parsec-scale jet of 3C279
- They attributed it to Faraday conversion requiring $\gamma_{\rm min} \lesssim 20$
- Combining this with the requirement that intrinsic Faraday rotation does not completely depolarize the jet then leads to mostly pair-plasma dominated jet
- However, Ruszkowski & Begelman later showed that a suitable turbulent B-field in a normal plasma can also reproduce the data

Comparing jet kinetic luminosities in pc and kpc scales

- Use synchrotron theory (plus δ estimates either from variability or from SSC) to calculate n_0 of the radiating electron population in parsec scales

Comparing jet kinetic luminosities in pc and kpc scales

- Use synchrotron theory (plus δ estimates either from variability or from SSC) to calculate n_0 of the radiating electron population in parsec scales
- $n = \int_{\gamma_{\rm min}}^{\gamma_{\rm max}} n_0 \gamma^{-p} d\gamma$, i.e., n depends heavily on $\gamma_{\rm min}$

Comparing jet kinetic luminosities in pc and kpc scales

- Use synchrotron theory (plus δ estimates either from variability or from SSC) to calculate n_0 of the radiating electron population in parsec scales
- $n = \int_{\gamma_{\min}}^{\gamma_{\max}} n_0 \gamma^{-p} d\gamma$, i.e., n depends heavily on $\gamma_{\min}$
- Kinetic luminosity is given by $L_{\rm kin} = \pi r_{\rm VLBI}^2 f n m_e c^2 \Gamma^2 \beta c \quad {\rm erg\,/s}$, where f contains the uncertainties about $\gamma_{\min}$ and matter content. $L_{\rm kin}$ becomes high for $e^- - p^+$ plasma unless $\gamma_{\min}$ is high.

Comparing jet kinetic luminosities in pc and kpc scales

- Use synchrotron theory (plus δ estimates either from variability or from SSC) to calculate n_0 of the radiating electron population in parsec scales
- $n = \int_{\gamma_{\rm min}}^{\gamma_{\rm max}} n_0 \gamma^{-p} d\gamma$, i.e., n depends heavily on $\gamma_{\rm min}$
- Kinetic luminosity is given by $L_{\rm kin} = \pi r_{\rm VLBI}^2 f n m_e c^2 \Gamma^2 \beta c \quad$ erg /s, where f contains the uncertainties about $\gamma_{\rm min}$ and matter content. $L_{\rm kin}$ becomes high for $e^- - p^+$ plasma unless $\gamma_{\rm min}$ is high.
- One can measure the power needed to fuel the kpc-scale structures and then compare this with $L_{\rm kin}$ in parsec scales. Provides limits on f and $\gamma_{\rm min}$.

Comparing jet kinetic luminosities in pc and kpc scales

- Use synchrotron theory (plus δ estimates either from variability or from SSC) to calculate n_0 of the radiating electron population in parsec scales
- $n = \int_{\gamma_{\rm min}}^{\gamma_{\rm max}} n_0 \gamma^{-p} d\gamma$, i.e., n depends heavily on $\gamma_{\rm min}$
- Kinetic luminosity is given by $L_{\rm kin} = \pi r_{\rm VLBI}^2 f n m_e c^2 \Gamma^2 \beta c$ erg /s, where f contains the uncertainties about $\gamma_{\rm min}$ and matter content. $L_{\rm kin}$ becomes high for $e^- - p^+$ plasma unless $\gamma_{\rm min}$ is high.
- One can measure the power needed to fuel the kpc-scale structures and then compare this with $L_{\rm kin}$ in parsec scales. Provides limits on f and $\gamma_{\rm min}$.
- Additional constraints from comparing particle flux with the limits from the accretion flow.

Comparing jet kinetic luminosities in pc and kpc scales

- Use synchrotron theory (plus δ estimates either from variability or from SSC) to calculate n_0 of the radiating electron population in parsec scales
- $n = \int_{\gamma_{\rm min}}^{\gamma_{\rm max}} n_0 \gamma^{-p} d\gamma$, i.e., n depends heavily on $\gamma_{\rm min}$
- Kinetic luminosity is given by $L_{\rm kin} = \pi r_{\rm VLBI}^2 f n m_e c^2 \Gamma^2 \beta c \quad$ erg /s, where f contains the uncertainties about $\gamma_{\rm min}$ and matter content. $L_{\rm kin}$ becomes high for $e^- - p^+$ plasma unless $\gamma_{\rm min}$ is high.
- One can measure the power needed to fuel the kpc-scale structures and then compare this with $L_{\rm kin}$ in parsec scales. Provides limits on f and $\gamma_{\rm min}$.
- Additional constraints from comparing particle flux with the limits from the accretion flow.
- Has produced mixed results regarding matter content